

© Théo Jalabert



# Rough volatility

Mathieu Rosenbaum

École Polytechnique

Fall 2020



- 1 Some elements about volatility modeling
- 2 Building the Rough FSV model
- 3 Application of the RFSV model : Volatility prediction
- 4 The microstructural foundations of rough volatility
- 5 Option pricing in the rough Heston model



- 1 Some elements about volatility modeling
- 2 Building the Rough FSV model
- 3 Application of the RFSV model : Volatility prediction
- 4 The microstructural foundations of rough volatility
- 5 Option pricing in the rough Heston model



Prices are often modeled as continuous semi-martingales of the form

$$dP_t = P_t(\mu_t dt + \sigma_t dW_t).$$

The volatility process  $\sigma_s$  is the most important ingredient of the model.  
Practitioners consider essentially three classes of volatility models :

- Deterministic volatility (Black and Scholes 1973),
- Local volatility (Dupire 1994),
- Stochastic volatility (Hull and White 1987, Heston 1993, Hagan et al. 2002,...).

In term of regularity, in these models, the volatility is either very smooth or with a smoothness similar to that of a Brownian motion.



To allow for a wider range of smoothness, we can consider the fractional Brownian motion in volatility modeling.

## Definition

The fractional Brownian motion (fBm) with Hurst parameter  $H$  is the only process  $W^H$  to satisfy :

- Self-similarity :  $(W_{at}^H) \stackrel{\mathcal{L}}{=} a^H(W_t^H)$ .
- Stationary increments :  $(W_{t+h}^H - W_t^H) \stackrel{\mathcal{L}}{=} (W_h^H)$ .
- Gaussian process with  $\mathbb{E}[W_1^H] = 0$  and  $\mathbb{E}[(W_1^H)^2] = 1$ .



## Proposition

For all  $\varepsilon > 0$ ,  $W^H$  is  $(H - \varepsilon)$ -Hölder a.s.

## Proposition

The absolute moments of the increments of the fBm satisfy

$$\mathbb{E}[|W_{t+h}^H - W_t^H|^q] = K_q h^{Hq}.$$

## Proposition

If  $H > 1/2$ , the fBm exhibits long memory in the sense that

$$\text{Cov}[W_{t+1}^H - W_t^H, W_1^H] \sim \frac{C}{t^{2-2H}}.$$



## Mandelbrot-van Ness representation

We have

$$W_t^H = \int_0^t \frac{dW_s}{(t-s)^{\frac{1}{2}-H}} + \int_{-\infty}^0 \left( \frac{1}{(t-s)^{\frac{1}{2}-H}} - \frac{1}{(-s)^{\frac{1}{2}-H}} \right) dW_s.$$



- Classical stochastic volatility models generate reasonable dynamics for the volatility surface.
- However they do not allow to fit the volatility surface, in particular the term structure of the ATM skew :

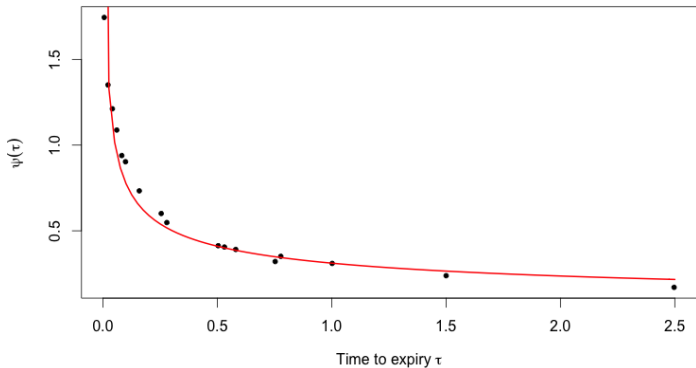
$$\psi(\tau) := \left| \frac{\partial}{\partial k} \sigma_{\text{BS}}(k, \tau) \right|_{k=0},$$

where  $k$  is the log-moneyness and  $\tau$  the maturity of the option.

# About option data : the volatility skew

© Theo Jalabert





The black dots are non-parametric estimates of the S&P ATM volatility skews as of June 20, 2013 ; the red curve is the power-law fit  
 $\psi(\tau) = A \tau^{-0.4}$ .

# About option data : fractional volatility

© Theo Jalabert



- The skew is well-approximated by a power-law function of time to expiry  $\tau$ . In contrast, conventional stochastic volatility models generate a term structure of ATM skew that is constant for small  $\tau$ .
- Models where the volatility is driven by a fBm generate an ATM volatility skew of the form  $\psi(\tau) \sim \tau^{H-1/2}$ , at least for small  $\tau$ .



- 1 Some elements about volatility modeling
- 2 Building the Rough FSV model
- 3 Application of the RFSV model : Volatility prediction
- 4 The microstructural foundations of rough volatility
- 5 Option pricing in the rough Heston model



We are interested in the dynamics of the (log)-volatility process. We use two proxies for the spot (squared) volatility of a day.

- A 5 minutes-sampling realized variance estimation taken over the whole trading day (8 hours).
- A one hour integrated variance estimator based on the model with uncertainty zones (Robert and R. 2012).

Note that we are not really considering a “spot” volatility but an “integrated” volatility. This might lead to some slight bias in our measurements (which can be controlled).

From now on, we consider realized variance estimations on the S&P over 3500 days, but the results are fairly “universal”.

# The log-volatility

© Théo Jalabert

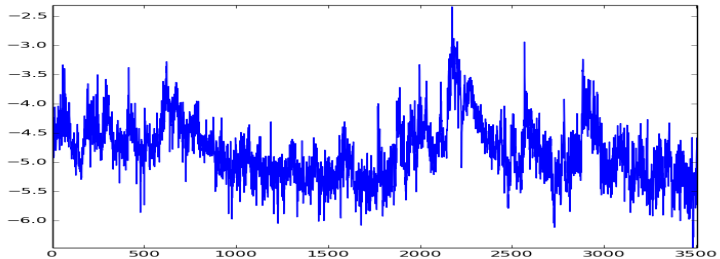


FIGURE – The log volatility  $\log(\sigma_t)$  as a function of  $t$ , S&P.

# Measure of the regularity of the log-volatility

©Theo Jalabert



The starting point of this work is to consider the scaling of the moments of the increments of the log-volatility. Thus we study the quantity

$$m(\Delta, q) = \mathbb{E}[|\log(\sigma_{t+\Delta}) - \log(\sigma_t)|^q],$$

or rather its empirical counterpart.

The behavior of  $m(\Delta, q)$  when  $\Delta$  is close to zero is related to the smoothness of the volatility (in the Hölder or even the Besov sense). Essentially, the regularity of the signal measured in  $L^q$  norm is  $s$  if  $m(\Delta, q) \sim c\Delta^{qs}$  as  $\Delta$  tends to zero.

# Scaling of the moments

© Théo Jalabert

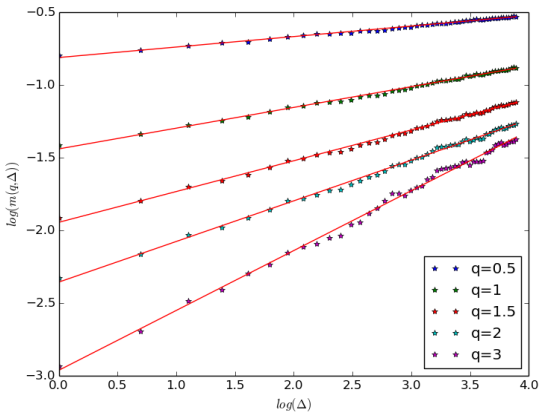


FIGURE –  $\log(m(q, \Delta)) = \zeta_q \log(\Delta) + C_q$ . The scaling is not only valid as  $\Delta$  tends to zero, but holds on a wide range of time scales.

# Monofractality of the log-volatility

© Théo Jalabert

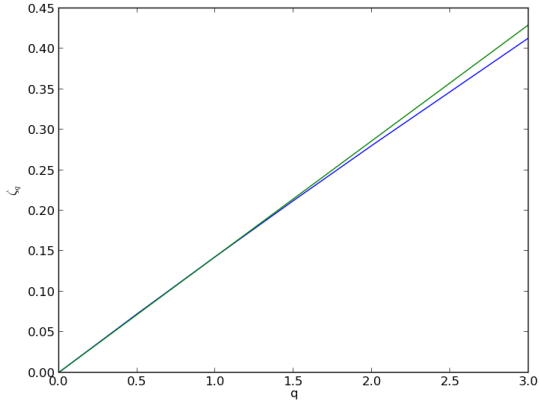


FIGURE – Empirical  $\zeta_q$  and  $q \rightarrow Hq$  with  $H = 0.14$  (similar to a fBm with Hurst parameter  $H$ ).

# Distribution of the log-volatility increments

© Theo Jäger

*Theo Jäger*

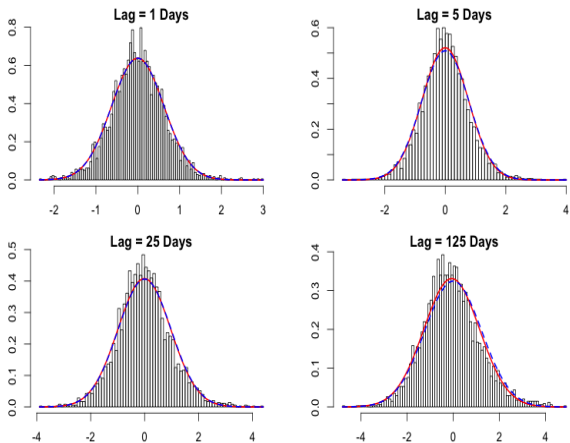


FIGURE – The distribution of the log-volatility increments is close to Gaussian.



## The RFSV model

These empirical findings suggest we model the log-volatility as a fractional Brownian motion :

$$\sigma_t = \sigma e^{\nu W_t^H}.$$



- An important property of volatility time series is their multiscaling behavior, see Mantegna and Stanley 2000 and Bouchaud and Potters 2003.
- This means one observes essentially the same law whatever the time scale.
- In particular, there are periods of high and low market activity at different time scales.
- Very few models reproduce this property, see multifractal models.

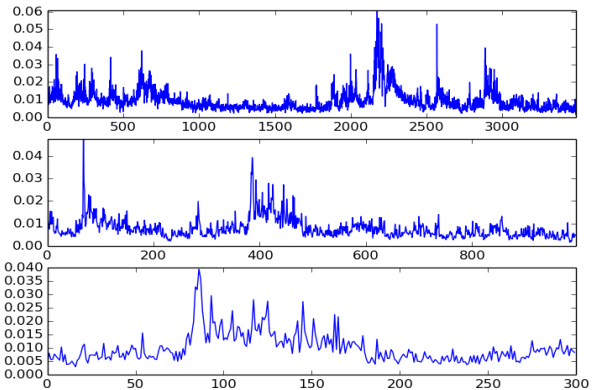
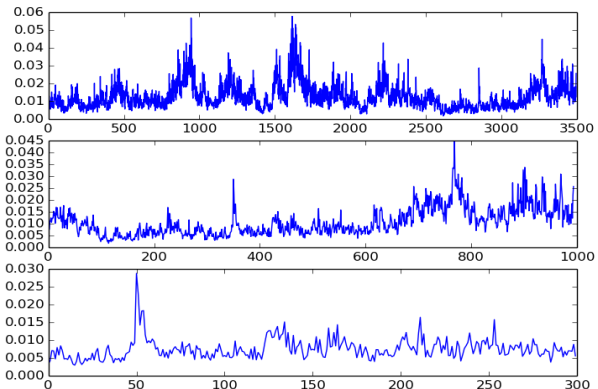


FIGURE – Empirical volatility over 10, 3 and 1 years.

# Our model on different time intervals

© Théo Jalabert



**FIGURE –** Simulated volatility over 10, 3 and 1 years. We observe the same alternations of periods of high market activity with periods of low market activity.

# Apparent multiscaling in our model

© Théo Jalabert



- Let  $L^{H,\nu}$  be the law on  $[0, 1]$  of the process  $e^{\nu W_t^H}$ .
- Then the law of the volatility process on  $[0, T]$  renormalized on  $[0, 1]$  :  $\sigma_{tT}/\sigma_0$  is  $L^{H,\nu T^H}$ .
- If one observes the volatility on  $T = 10$  years (2500 days) instead of  $T = 1$  day, the parameter  $\nu T^H$  defining the law of the volatility is only multiplied by  $2500^H \sim 3$ .
- Therefore, one observes quite the same properties on a very wide range of time scales.
- The roughness of the volatility process ( $H = 0.14$ ) implies a multiscaling behavior of the volatility.



- 1 Some elements about volatility modeling
- 2 Building the Rough FSV model
- 3 Application of the RFSV model : Volatility prediction
- 4 The microstructural foundations of rough volatility
- 5 Option pricing in the rough Heston model



There is a nice prediction formula for the fractional Brownian motion.

## Proposition (Nuzman and Poor 2000)

For  $H < 1/2$

$$\mathbb{E}[W_{t+\Delta}^H | \mathcal{F}_t] = \frac{\cos(H\pi)}{\pi} \Delta^{H+1/2} \int_{-\infty}^t \frac{W_s^H}{(t-s+\Delta)(t-s)^{H+1/2}} ds.$$

# Our prediction formula

© Théo Jalabert



We apply the previous formula to the prediction of the log-volatility :

$$\mathbb{E} [\log \sigma_{t+\Delta}^2 | \mathcal{F}_t] = \frac{\cos(H\pi)}{\pi} \Delta^{H+1/2} \int_{-\infty}^t \frac{\log \sigma_s^2}{(t-s+\Delta)(t-s)^{H+1/2}} ds$$

or more precisely its discrete version :

$$\mathbb{E} [\log \sigma_{t+\Delta}^2 | \mathcal{F}_t] = \frac{\cos(H\pi)}{\pi} \Delta^{H+1/2} \sum_{k=0}^N \frac{\log \sigma_{t-k}^2}{(k + \Delta + 1/2)(k + 1/2)^{H+1/2}}.$$

We compare it to usual predictors using the criterion

$$P = \frac{\sum_{k=1}^{N-\Delta} (\widehat{\log(\sigma_{k+\Delta}^2)} - \log(\sigma_{k+\Delta}^2))^2}{\sum_{k=1}^{N-\Delta} (\log(\sigma_{k+\Delta}^2) - \mathbb{E}[\log(\sigma_{t+\Delta}^2)])^2}.$$

	AR(5)	AR(10)	HAR(3)	RFSV
SPX2.rv $\Delta = 1$	0.317	0.318	0.314	<b>0.313</b>
SPX2.rv $\Delta = 5$	0.459	0.449	0.437	<b>0.426</b>
SPX2.rv $\Delta = 20$	0.764	0.694	0.656	<b>0.606</b>
FTSE2.rv $\Delta = 1$	0.230	0.229	0.225	<b>0.223</b>
FTSE2.rv $\Delta = 5$	0.357	0.344	0.337	<b>0.320</b>
FTSE2.rv $\Delta = 20$	0.651	0.571	0.541	<b>0.472</b>
N2252.rv $\Delta = 1$	0.357	0.358	0.351	<b>0.345</b>
N2252.rv $\Delta = 5$	0.553	0.533	0.513	<b>0.504</b>
N2252.rv $\Delta = 20$	0.875	0.795	0.746	<b>0.714</b>
GDAXI2.rv $\Delta = 1$	0.237	0.238	0.234	<b>0.231</b>
GDAXI2.rv $\Delta = 5$	0.372	0.362	0.350	<b>0.339</b>
GDAXI2.rv $\Delta = 20$	0.661	0.590	0.550	<b>0.498</b>
FCHI2.rv $\Delta = 1$	0.244	0.244	0.241	<b>0.238</b>
FCHI2.rv $\Delta = 5$	0.378	0.373	0.366	<b>0.350</b>
FCHI2.rv $\Delta = 20$	0.669	0.613	0.598	<b>0.522</b>



After a simple change of variable, the prediction of the log-volatility can be written :

$$\mathbb{E}[\log(\sigma_{t+\Delta}^2) | \mathcal{F}_t] \sim \frac{\cos(H\pi)}{\pi} \int_0^1 \frac{\log(\sigma_{t-\Delta u}^2)}{(u+1) u^{H+1/2}} du.$$

The only time scale that appears in the above regression is the horizon  $\Delta$ .

As it is known by practitioners :

*If trying to predict volatility one week ahead, one should essentially look at the volatility over the last week. If trying to predict the volatility one month ahead, one should essentially look at the volatility over the last month.*

# Conditional distribution of the fractional Brownian motion and prediction of the variance

© Theo Jalabert



## Proposition (Nuzman and Poor 2000)

In law,

$$W_{t+\Delta}^H | \mathcal{F}_t = \mathcal{N}(\mathbb{E}[W_{t+\Delta}^H | \mathcal{F}_t], c\Delta^{2H})$$

with

$$c = \frac{\sin(\pi(1/2 - H))\Gamma(3/2 - H)^2}{\pi(1/2 - H)\Gamma(2 - 2H)}.$$

Therefore, our predictor of the variance writes :

$$\mathbb{E}[\sigma_{t+\Delta}^2 | \mathcal{F}_t] = e^{\mathbb{E}[\log(\sigma_{t+\Delta}^2) | \mathcal{F}_t] + 2\nu^2 c\Delta^{2H}}.$$

	AR(5)	AR(10)	HAR(3)	RFSV
SPX2.rv $\Delta = 1$	0.520	0.566	0.489	<b>0.475</b>
SPX2.rv $\Delta = 5$	0.750	0.745	0.723	<b>0.672</b>
SPX2.rv $\Delta = 20$	1.070	1.010	1.036	<b>0.903</b>
FTSE2.rv $\Delta = 1$	0.612	0.621	0.582	<b>0.567</b>
FTSE2.rv $\Delta = 5$	0.797	0.770	0.756	<b>0.707</b>
FTSE2.rv $\Delta = 20$	1.046	0.984	0.935	<b>0.874</b>
N2252.rv $\Delta = 1$	0.554	0.579	<b>0.504</b>	0.505
N2252.rv $\Delta = 5$	0.857	0.807	0.761	<b>0.729</b>
N2252.rv $\Delta = 20$	1.097	1.046	1.011	<b>0.964</b>
GDAXI2.rv $\Delta = 1$	0.439	0.448	0.399	<b>0.386</b>
GDAXI2.rv $\Delta = 5$	0.675	0.650	0.616	<b>0.566</b>
GDAXI2.rv $\Delta = 20$	0.931	0.850	0.816	<b>0.746</b>
FCHI2.rv $\Delta = 1$	0.533	0.542	0.470	<b>0.465</b>
FCHI2.rv $\Delta = 5$	0.705	0.707	0.691	<b>0.631</b>
FCHI2.rv $\Delta = 20$	0.982	0.952	0.912	<b>0.828</b>



- 1 Some elements about volatility modeling
- 2 Building the Rough FSV model
- 3 Application of the RFSV model : Volatility prediction
- 4 The microstructural foundations of rough volatility
- 5 Option pricing in the rough Heston model



## Summary of what we have seen and objectives

- We know that : **Volatility is rough !**
- On any asset, using any reasonable volatility proxy/statistical method (realized volatility, realized kernels, uncertainty zones, Garman-Klass, implied volatility, power variations, autocorrelations, Whittle,...), one concludes that volatility is rough.
- It cannot be just coincidence...
- We want to show that typical behaviors of market participants at the high frequency scale naturally lead to rough volatility.
- Our modeling tool : **Hawkes processes.**

## Hawkes process

- A Hawkes process  $(N_t)_{t \geq 0}$  is a self-exciting point process, whose intensity at time  $t$ , denoted by  $\lambda_t$ , is of the form

$$\lambda_t = \mu + \sum_{0 < J_i < t} \phi(t - J_i) = \mu + \int_{(0,t)} \phi(t - s) dN_s,$$

where  $\mu$  is a positive real number,  $\phi$  a regression kernel and the  $J_i$  are the points of the process before time  $t$ .

- These processes have been introduced in 1971 by Hawkes in the purpose of modeling earthquakes and their aftershocks.



## Order flow and volatility

- Thus, it is nowadays classical to model the order flow (number of trades) thanks to Hawkes processes.
- It is known from financial economics theory (see for example Madhavan, Richardson and Roomans (97)) that the order flow is essentially the same thing as the integrated volatility (variance) if the time scale is large enough :

$$N_t \approx \int_0^t \sigma^2(s) ds.$$



## Two main reasons for the popularity of Hawkes processes

- These processes represent a very natural and tractable extension of Poisson processes. In fact, comparing point processes and conventional time series, Poisson processes are often viewed as the counterpart of iid random variables whereas Hawkes processes play the role of autoregressive processes.
- Another explanation for the appeal of Hawkes processes is that it is often easy to give a convincing interpretation to such modeling. To do so, the branching structure of Hawkes processes is quite helpful.



## Poisson cluster representation

- Under the assumption  $\|\phi\|_1 < 1$ , where  $\|\phi\|_1$  denotes the  $L^1$  norm of  $\phi$ , Hawkes processes can be represented as a population process where migrants arrive according to a Poisson process with parameter  $\mu$ .
- Then each migrant gives birth to children according to a non homogeneous Poisson process with intensity function  $\phi$ , these children also giving birth to children according to the same non homogeneous Poisson process, see Hawkes (74).
- Now consider for example the classical case of buy (or sell) market orders. Then migrants can be seen as exogenous orders whereas children are viewed as orders triggered by other orders.



## The condition $\|\phi\|_1 < 1$

- The assumption  $\|\phi\|_1 < 1$  is crucial in the study of Hawkes processes.
- If one wants to get a stationary intensity with finite first moment, then the condition  $\|\phi\|_1 < 1$  is required (similar condition as for the AR(1) process).
- This condition is also necessary in order to obtain classical ergodic properties for the process.
- For these reasons, this condition is often called stability condition in the Hawkes literature.



## Degree of endogeneity of the market

- From a practical point of view, a lot of interest has been recently devoted to the parameter  $\|\phi\|_1$ .
- For example, Hardiman, Bercot and Bouchaud (13) and Filimonov and Sornette (12,13) use the branching interpretation of Hawkes processes on midquote data in order to measure the so-called degree of endogeneity of the market, defined by  $\|\phi\|_1$ .



## Degree of endogeneity of the market

- The parameter  $\|\phi\|_1$  corresponds to the average number of children of an individual,  $\|\phi\|_1^2$  to the average number of grandchildren of an individual, ... Therefore, if we call cluster the descendants of a migrant, then the average size of a cluster is given by  $\sum_{k \geq 1} \|\phi\|_1^k = \|\phi\|_1 / (1 - \|\phi\|_1)$ .
- Thus, the average proportion of endogenously triggered events is  $\|\phi\|_1 / (1 - \|\phi\|_1)$  divided by  $1 + \|\phi\|_1 / (1 - \|\phi\|_1)$ , which is equal to  $\|\phi\|_1$ .



## Unstable Hawkes processes

- This branching ratio can be measured using parametric and non-parametric estimation methods for Hawkes processes, see Ogata (78,83) for likelihood based methods and Reynaud-Bouret and Schbath (10) and Al Dayri *et al.* (11) for functional estimators of the function  $\phi$ .
- In Hardiman, Bercot and Bouchaud (13), very stable estimations of  $\|\phi\|_1$  are reported for the E-mini S&P futures between 1998 and 2012, the results being systematically close to one.
- This is also the case for Bund and Dax futures in Al Dayri *et al.* (11) and various other assets in Filimonov and Sornette (12).

## Limiting behavior of Hawkes processes

- Our aim is to study the behavior at large time scales of so-called **nearly unstable Hawkes processes**, which correspond to these estimations of  $\|\phi\|_1$ , close to 1.
- This will give us insights on the properties of the integrated volatility.
- Furthermore, we want to take into account another stylized fact : The function  $\phi$  has typically a power law tail :

$$\phi(x) \underset{x \rightarrow +\infty}{\sim} \frac{K}{x^{1+\alpha}},$$

with  $\alpha$  of order 0.5-0.7.

- This memory effect is likely due to metaorders splitting.

## Sequence of Hawkes processes

- We consider a sequence of Hawkes processes  $(N_t^T)_{t \geq 0}$  indexed by  $T \rightarrow \infty$  with

$$\lambda_t^T = \mu^T + \int_0^t \phi^T(t-s)dN_s^T.$$

- For some sequence  $a_T < 1$ ,  $a_T \rightarrow 1$ ,  $K > 0$  and  $\alpha \in (0, 1)$  :

$$\phi^T(t) = a_T \phi(t), \quad \alpha x^\alpha (1 - F(x)) \xrightarrow{x \rightarrow +\infty} K,$$

with  $\|\phi\|_1 = 1$  and

$$F(x) = \int_0^x \phi(s)ds.$$

## Martingale process

- Let  $M^T$  be the martingale process associated to  $N^T$ , that is, for  $t \geq 0$ ,

$$M_t^T = N_t^T - \int_0^t \lambda_s^T ds.$$

- We also set  $\psi^T$  the function defined on  $\mathbb{R}^+$  by

$$\psi^T(t) = \sum_{k=1}^{\infty} (\phi^T)^{*k}(t).$$

- We can show that

$$\lambda_t^T = \mu^T + \int_0^t \psi^T(t-s) \mu^T ds + \int_0^t \psi^T(t-s) dM_s^T.$$

## Rescaling

- We rescale our processes so that they are defined on  $[0, 1]$ . To do that, we consider for  $t \in [0, 1]$

$$\lambda_{tT}^T = \mu^T + \int_0^{tT} \psi^T(Tt - s) \mu^T ds + \int_0^{tT} \psi^T(Tt - s) dM_s^T.$$

- For the scaling in space, a natural multiplicative factor is  $(1 - a_T)/\mu^T$ . Indeed, in the stationary case,

$$\mathbb{E}[\lambda_t^T] = \mu^T / (1 - \|\phi^T\|_1).$$

Thus, the order of magnitude of the intensity is  $\mu^T(1 - a_T)^{-1}$ . This is why we define

$$C_t^T = \lambda_{tT}^T(1 - a_T)/\mu^T.$$

## Decomposition of $C_t^T$

- Then we easily get :

$$C_t^T = (1 - a_T) + \int_0^t T(1 - a_T)\psi^T(Ts)ds + \sqrt{\frac{T(1 - a_T)}{\mu^T}} \int_0^t \psi^T(T(t-s))\sqrt{C_s^T} dB_s^T,$$

with

$$B_t^T = \frac{1}{\sqrt{T}} \int_0^{tT} \frac{dM_s^T}{\sqrt{\lambda_s^T}}.$$

## The function $\psi^T$

- The asymptotic behavior of  $C_t^T$  is closely linked to that of  $\psi^T$ .
- Remark that the function defined for  $x \geq 0$  by

$$\rho^T(x) = T \frac{\psi^T(Tx)}{\|\psi^T\|_1}$$

is the density of the random variable

$$X^T = \frac{1}{T} \sum_{i=1}^{I^T} X_i,$$

where the  $(X_i)$  are iid random variables with density  $\phi$  and  $I^T$  is a geometric random variable with parameter  $1 - a_T$ .

# Non-degenerate limit for nearly unstable Hawkes processes

© Theo Jalabert



## The function $\psi^T$

- The Laplace transform of the random variable  $X^T$ , denoted by  $\hat{\rho}^T$ , satisfies :

$$\hat{\rho}^T(z) = \frac{\hat{\phi}\left(\frac{z}{T}\right)}{1 - \frac{a_T}{1-a_T}(\hat{\phi}\left(\frac{z}{T}\right) - 1)},$$

where  $\hat{\phi}$  denotes the Laplace transform of  $X_1$ .

- Due to the assumptions on  $\phi$ , we have

$$\hat{\phi}(z) = 1 - K \frac{\Gamma(1-\alpha)}{\alpha} z^\alpha + o(z^\alpha).$$

## The function $\psi^T$

- Set  $\delta = K \frac{\Gamma(1-\alpha)}{\alpha}$  and  $v_T = \delta^{-1} T^\alpha (1 - a_T)$ .
- Using that  $a_T$  and  $\hat{\phi}(\frac{z}{T})$  both tend to 1 as  $T$  goes to infinity,  $\hat{\rho}^T(z)$  is equivalent to

$$\frac{v_T}{v_T + z^\alpha}.$$

- The function whose Laplace transform is equal to this last quantity is given by

$$v_T x^{\alpha-1} E_{\alpha,\alpha}(-v_T x^\alpha),$$

with  $E_{\alpha,\beta}$  the  $(\alpha, \beta)$  Mittag-Leffler function.



## Expected limit for $C_t^T$

- Putting everything together, we can expect (for  $\alpha > 1/2$ )

$$C_t^T \sim v_T \int_0^t s^{\alpha-1} E_{\alpha,\alpha}(-v_T s^\alpha) ds + \gamma_T v_T \int_0^t (t-s)^{\alpha-1} E_{\alpha,\alpha}(-v_T(t-s)^\alpha) \sqrt{C_s^T} dB_s^T,$$

with

$$\gamma_T = \frac{1}{\sqrt{\mu^T T(1-a_T)}}.$$

- The process  $B^T$  can be shown to converge to a Brownian motion  $B$ .

## Expected limit for $C_t^T$

- We need that both  $v_T$  and  $\gamma_T$  converge to positive constants so we assume :

$$T^\alpha(1 - a_T) \rightarrow \lambda\delta, \quad T^{1-\alpha}\mu^T \rightarrow \mu^*\delta^{-1}.$$

- Passing to the limit, we obtain (for  $\alpha > 1/2$ )

$$\begin{aligned} C_t^\infty &\sim \lambda \int_0^t s^{\alpha-1} E_{\alpha,\alpha}(-\lambda s^\alpha) ds \\ &\quad + \sqrt{\frac{\lambda}{\mu^*}} \int_0^t (t-s)^{\alpha-1} E_{\alpha,\alpha}(-\lambda(t-s)^\alpha) \sqrt{C_s^\infty} dB_s. \end{aligned}$$



## Limit theorem

For  $\alpha > 1/2$ , the sequence of renormalized Hawkes processes converges to some process which is differentiable on  $[0, 1]$ . Moreover, the law of its derivative  $V$  satisfies

$$V_t = F^{\alpha, \lambda}(t) + \frac{1}{\sqrt{\mu^* \lambda}} \int_0^t f^{\alpha, \lambda}(t-s) \sqrt{V_s} dB_s^1,$$

with  $B^1$  a Brownian motion and

$$f^{\alpha, \lambda}(x) = \lambda x^{\alpha-1} E_{\alpha, \alpha}(-\lambda x^\alpha).$$

## Rough Heston model

Using fractional integration, we easily get that the equation for  $V_t$  on the preceding slide is equivalent to

$$V_t = \frac{1}{\Gamma(\alpha)} \int_0^t (t-s)^{\alpha-1} \lambda (1 - V_s) ds + \frac{1}{\Gamma(\alpha)} \sqrt{\frac{\lambda}{\mu^*}} \int_0^t (t-s)^{\alpha-1} \sqrt{V_s} dB_s.$$

Now recall Mandelbrot-van-Ness representation :

$$W_t^H = \int_0^t \frac{dW_s}{(t-s)^{\frac{1}{2}-H}} + \int_{-\infty}^0 \left( \frac{1}{(t-s)^{\frac{1}{2}-H}} - \frac{1}{(-s)^{\frac{1}{2}-H}} \right) dW_s.$$

Therefore we have a rough Heston model with  $H = \alpha - 1/2$ . Furthermore, for any  $\varepsilon > 0$ ,  $Y$  has Hölder regularity  $\alpha - 1/2 - \varepsilon$ .



## Microstructural foundations for the RFSV model

- It is clearly established that there is a linear relationship between cumulated order flow and integrated variance.
- Consequently the “derivative” of the order flow corresponds to the spot variance.
- Thus endogeneity of the market together with order splitting lead to a superposition effect which explains (at least partly) the rough nature of the observed volatility.
- Near instability together with a tail index  $\alpha \sim 0.6$  correspond to  $H \sim 0.1$ .
- In fact one can show that rough volatility is just a consequence of the no statistical arbitrage principle.



- 1 Some elements about volatility modeling
- 2 Building the Rough FSV model
- 3 Application of the RFSV model : Volatility prediction
- 4 The microstructural foundations of rough volatility
- 5 Option pricing in the rough Heston model

# Deriving the characteristic function of the rough Heston model

© Theo Jalabert



## Strategy

- Modifying slightly our last theorem, we are able to derive the characteristic function of a high frequency price model converging towards the rough Heston model.
- We then pass to the limit.



We write :

$$I^{1-\alpha}f(x) = \frac{1}{\Gamma(1-\alpha)} \int_0^x \frac{f(t)}{(x-t)^\alpha} dt, \quad D^\alpha f(x) = \frac{d}{dx} I^{1-\alpha}f(x).$$

## Theorem

The characteristic function at time  $t$  for the rough Heston model is given by

$$\exp\left(\int_0^t g(a, s) ds + \frac{V_0}{\theta\lambda} I^{1-\alpha}g(a, t)\right),$$

with  $g(a, )$  the unique solution of the fractional Riccati equation :

$$D^\alpha g(a, s) = \frac{\lambda\theta}{2}(-a^2 - ia) + \lambda(i a \rho \nu - 1)g(a, s) + \frac{\lambda\nu^2}{2\theta}g^2(a, s).$$



We collect S&P implied volatility surface, from Bloomberg, for different maturities

$$T_j = 0.25, 0.5, 1, 1.5, 2 \text{ years},$$

and different moneyness

$$K/S_0 = 0.80, 0.90, 0.95, 0.975, 1.00, 1.025, 1.05, 1.10, 1.20.$$

Calibration results on data of 7 January 2010 :

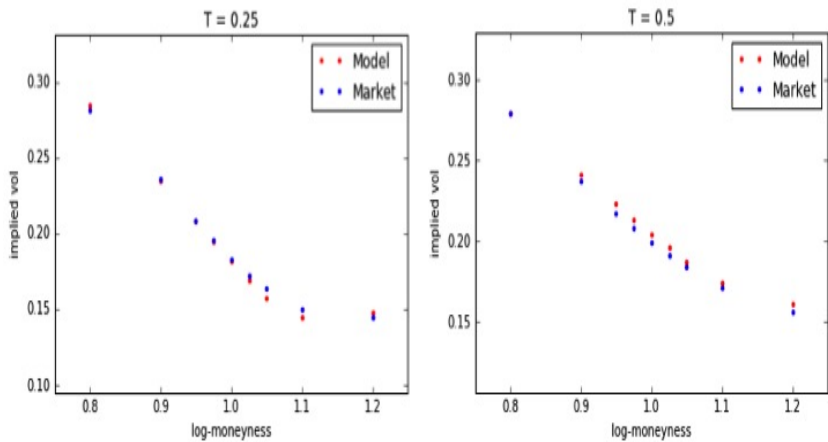
$$\rho = -0.68; \quad \nu = 0.305; \quad H = 0.09.$$

# Calibration results : Market vs model implied volatilities, 7

January 2010

© Theo Jalabert

Theo Jalabert

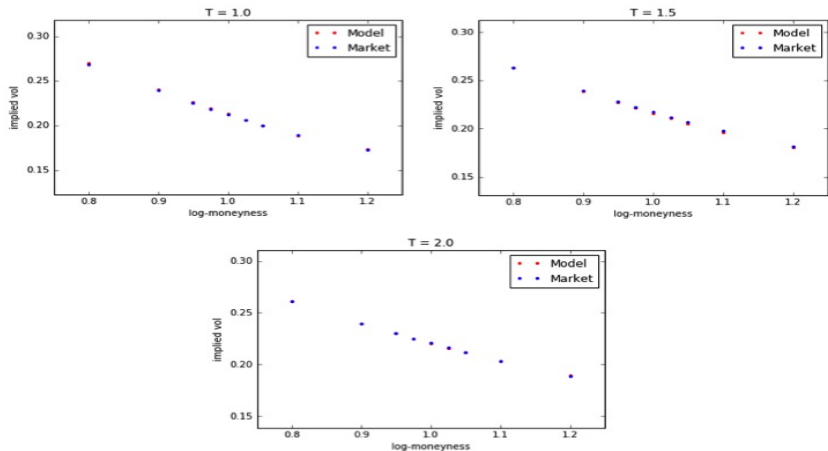


# Calibration results : Market vs model implied volatilities, 7

January 2010

© Theo Jalabert

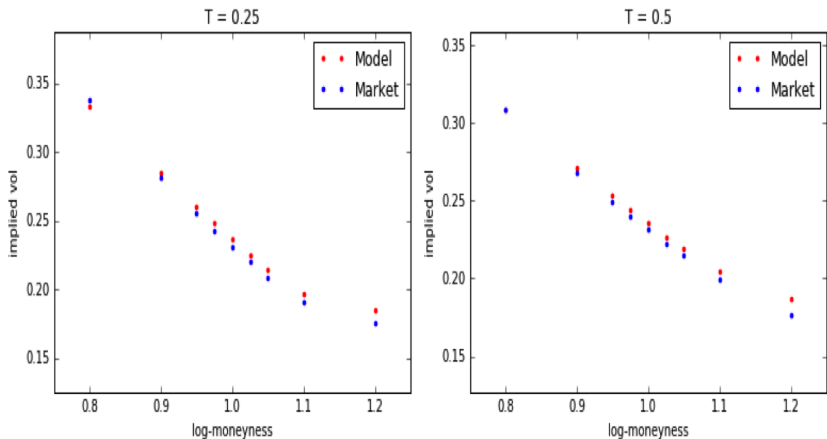
Theo Jalabert



# Stability : Results on 8 February 2010 (one month after calibration)

© Théo Jalabert

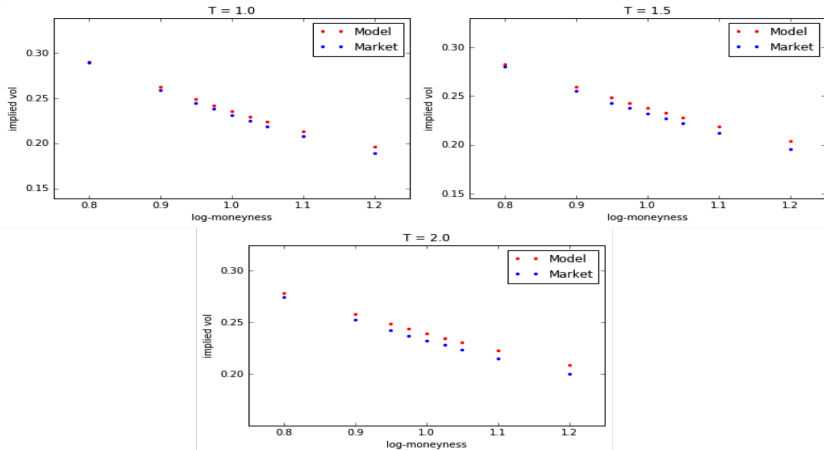




# Stability : Results on 8 February 2010 (one month after calibration)

© Théo Jalabert

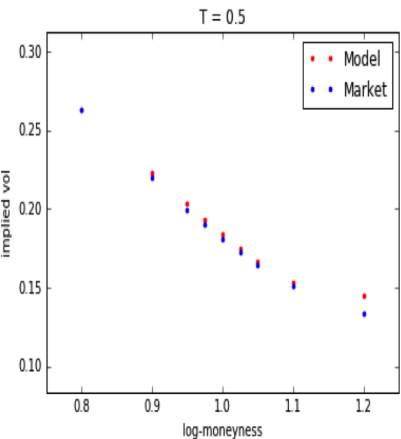
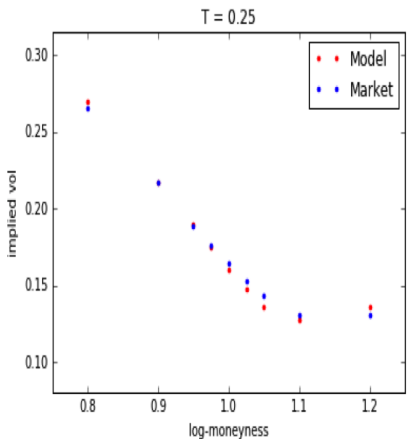




# Stability : Results on 7 April 2010 (three months after calibration)

© Theo Jalabert

Theo Jalabert



# Stability : Results on 7 April 2010 (three months after calibration)

© Theo Jalabert

Theo Jalabert

